Near-infrared fluorescence imaging in colorectal cancer and its metastases

Meijer, R.P.J.

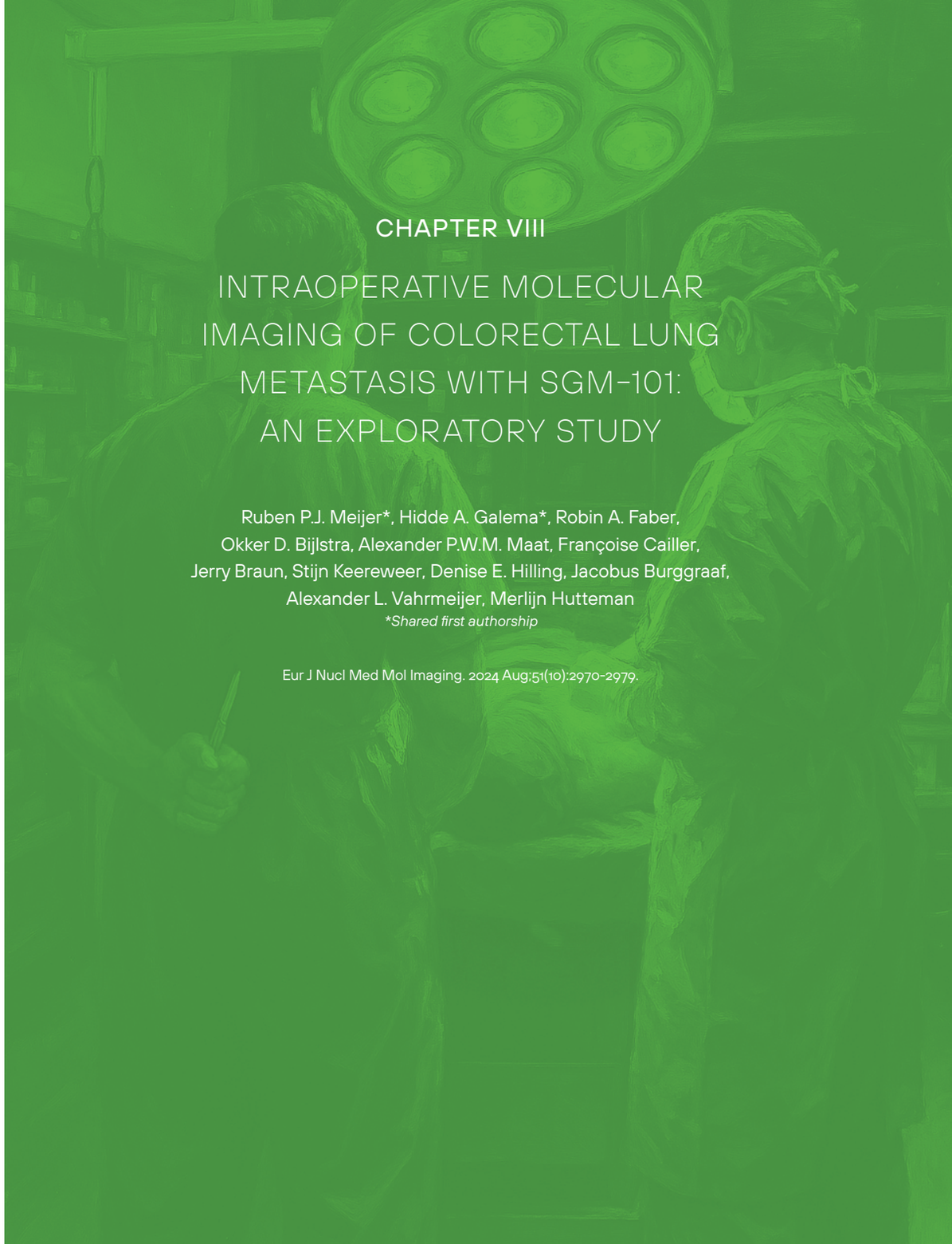

CHAPTER VIII

INTRAOPERATIVE MOLECULAR IMAGING OF COLORECTAL LUNG METASTASIS WITH SGM-101: AN EXPLORATORY STUDY

Ruben P.J. Meijer*, Hidde A. Galema*, Robin A. Faber, Okker D. Bijlstra, Alexander P.W.M. Maat, Françoise Cailler, Jerry Braun, Stijn Keereweer, Denise E. Hilling, Jacobus Burggraaf, Alexander L. Vahrmeijer, Merlijn Hutteman

**Shared first authorship*

Eur J Nucl Med Mol Imaging. 2024 Aug;51(10):2970-2979.

Abstract

PURPOSE Metastasectomy is a common treatment option for patients with colorectal lung metastases (CLM). Challenges exist with margin assessment and identification of small nodules, especially during minimally invasive surgery. Intraoperative fluorescence imaging has the potential to overcome these challenges. The aim of this study was to assess feasibility of targeting CLM with the carcinoembryonic antigen (CEA) specific fluorescent tracer SGM-101.

METHODS This was a prospective, open-label feasibility study. The primary outcome was the number of CLM that showed a true positive fluorescence signal with SGM-101. Fluorescence positive signal was defined as a signal-to-background ratio (SBR) ≥ 1.5. A secondary endpoint was the CEA expression in the colorectal lung metastases, assessed with the immunohistochemistry and scored by the total immunostaining score.

RESULTS Thirteen patients were included in this study. Positive fluorescence signal with *in vivo*, back table and closed-field bread loaf imaging was observed in 31%, 45% and 94% of the tumours respectively. Median SBRs for the three imaging modalities were 1.00 (IQR: 1.00-1.53), 1.45 (IQR: 1.00-1.89) and 4.81 (IQR: 2.70-7.41). All tumour lesions had a maximum total immunostaining score for CEA expression of 12/12.

CONCLUSION This study demonstrated the potential of fluorescence imaging of CLM with SGM-101. CEA expression was observed in all tumours and closed-field imaging showed excellent CEA specific targeting of the tracer to the tumour nodules. The full potential of SGM-101 for *in vivo* detection of the tracer can be achieved with improved minimal invasive imaging systems and optimal patient selection.

Introduction

Around 5% of the patients with colorectal cancer (CRC) develop lung metastases after treatment with curative intent.[1,2] For selected, oligo-metastatic patients, metastasectomy is an important treatment option so long as the primary disease is under control. Tumour identification during metastasectomy is sometimes challenging, as nodules can be small. Positive margins are associated with decreased overall survival, which makes complete removal of the tumour of utmost importance.[3] While the introduction of video-assisted thoracic surgery (VATS) has reduced surgical morbidity, tumour identification has become more challenging. Therefore, interest is growing in other methods for intraoperative detection of colorectal lung metastases (CLM).

Intraoperative, tumour-specific, near-infrared (NIR) fluorescence imaging is developed for several surgical procedures, including lung surgery.[4] To realize NIR fluorescence tumour imaging, patients are administered intravenously with a tumour-specific tracer attached to a fluorophore. Imaging of these agents with a fluorescence imaging system allows for real-time intraoperative visualization of the tumour.[5] SGM-101 is a fluorescent tracer that consists of a monoclonal antibody that targets carcinoembryonic antigen (CEA), labelled with a NIR fluorophore (BM-104). This fluorophore has an excitation and emission wavelength around 700 nm.[6] CEA is overexpressed in >95% of the colorectal cancers and thus an excellent target for molecular imaging of CRC.[7] NIR fluorescence imaging of CLM with SGM-101 may improve intraoperative detection of these tumours and thus increase the chance of a complete resection of the tumour.

Intraoperative NIR fluorescence imaging with SGM-101 has been studied in trials for locally advanced CRC, peritoneal metastases of CRC, colorectal liver metastases, and pancreatic cancer.[8-12] In a phase II rectal cancer trial, NIR fluorescence imaging with SGM-101 resulted in a change in surgical plan in 7 out of 37 patients. Currently, two phase III trials are ongoing with SGM-101 for CRC and peritoneal metastases.[13,14] The aim of this study was to assess the potential of targeting CLM with SGM-101.

Methods

This study was reviewed and approved by the medical ethical committee 'Leiden-Den Haag-Delft' and conducted according to the declaration of Helsinki (10th version, Fortaleza, 2013). Informed consent was obtained from all

study participants. The study was registered in Clinicaltrials.gov under identifier NCT04737213. The study was conducted in the Leiden University Medical Center (LUMC) and the Erasmus MC Cancer Institute (EMC).

STUDY DESIGN

This was a prospective, open-label, non-randomized feasibility study to assess the ability of SGM-101 to target CLM. In this single arm trial, all patients were intravenously administered with SGM-101. SGM-101 was supplied by Surgimab (Montpellier, France). All patients received intravenous administration three to five days prior to surgery, based on earlier study protocols.[10–12] The drug was administered over 30 minutes and patients were observed for three hours after infusion. Patients at least 18 years old, scheduled for resection of (suspected) CLM, and willing and able to give written informed consent were eligible for inclusion. Exclusion criteria were: history of any anaphylactic reaction, other malignancies either currently active or diagnosed in the last 5 years, hepatic or renal insufficiencies, blood count abnormalities, known positive test for HIV, hepatitis B surface antigen or hepatitis C virus antibody or patients with untreated serious infections, patients pregnant or breastfeeding, or any condition that the investigator considered to be potentially jeopardizing the patient's wellbeing or the study objectives.

OUTCOMES

The primary outcome of this study was the number of CLM that showed a true positive fluorescence signal with SGM-101 and a NIR fluorescence imaging system. Secondary endpoints were the optimal dose of SGM-101 for fluorescence imaging of CLM, possible change in surgical management based on fluorescence imaging, and concordance between fluorescence imaging and CEA expression on the corresponding tissue slides.

For the primary outcome, lesions were considered fluorescent (i.e. a positive index test) if the signal-to-background ratio (SBR) was ≥ 1.5.[15] The reference standard for demonstrating CLM was final histopathological assessment. Imaging of the CLM was performed in three settings: *in vivo* imaging, *ex vivo* imaging of the whole specimen on the back table (back table imaging), and *ex vivo* imaging of bread loaf slides in a closed-field imaging device (closed-field imaging). *In vivo* and back table imaging was performed with the Quest spectrum V2 fluorescence camera (Middenmeer, The Netherlands). During VATS, the endoscopic camera of Quest spectrum V2 was used. Closed-field imaging was performed with the PEARL MSI imaging system (Li-Cor ,Lincoln, Nebraska, USA). SBRs were calculated with the 'Quest TBR tool' (Quest Medical Imaging, Middenmeer, The Netherlands) and Image Studio software (Li-Cor, Lincoln, Nebraska, USA). The SBR was defined as the mean fluorescence intensity of the signal derived from the tumour divided by the mean fluorescence intensity of the surrounding normal tissue.

Doses of 7.5, 10, and 12.5 mg were studied. The optimal dose was decided based on closed-field bread loaf imaging. As this was a feasibility study, no direct change in surgical management was performed, based on intraoperative fluorescence imaging alone. However, possible change in surgical management was noted as a secondary outcome measure (type D study).[16] CEA expression was assessed by immunohistochemistry with the monoclonal mouse antibody against CEACAM5 (clone number CI-P83-1, Santa Cruz Biotechnology).[12] Scoring of staining was done by multiplying the intensity score by the proportion score, to calculate the total immunostaining score (TIS).[17] A dedicated pathologist (MD) performed scoring of the immunohistochemistry-stained tissue slides.

STATISTICS

R software (version 4.1.0, R Foundation for statistical computing, Vienna, Austria) was used for statistical analysis. Numerical data was described with median and interquartile range (IQR) or range. To assess SBR differences between dose groups, a Kruskal-Wallis test was performed. To assess the influence of overlying lung parenchyma on fluorescence signal intensity, tumours were categorized as closer or further distanced than 14 mm of the visceral pleura as defined by pre-operative computed tomography (CT). anti-CEACAM5 [18] $P < 0.05$ was considered significant. The sample size is based upon experience with this type of compounds and not on a formal power calculation. Using the 3+3 dose escalation design, a minimum of 9 and a maximum of 15 patients will be included, corresponding to a minimum of 3 patients per dose level. Patients were allocated in a chronological order.

Results

Between January 2021 and September 2022, 13 patients (ten males, three females) with a median age of 56 years (IQR: 54.5-66.5) were included. Patient and surgical characteristics are described in Table 1. There were no (serious) adverse events with any possible relationship to the administration of SGM-101.

TABLE 1 Patient- and surgical characteristics.

		N (%)*
Patients		13 (100)
Sex	Male	10 (77)
	Female	3 (23)
Hospital	LUMC	7 (46)
	EMC	6 (54)
Age (median [IQR])		56 [54.5-66.5]
Serum CEA (µg/ml) (median [IQR])		5.8 [3.33-8.5]
Location metastasis	RUL	5 (28)
	ML	1 (6)
	RLL	6 (33)
	LUL	3 (17)
	LLL	3 (17)
Surgical procedure**	Lobectomy	4 (31)
	Segment resection	2 (15)
	Wedge resection	9 (69)
	Lymphadenectomy	5 (38)
Surgical approach	Thoracotomy	2 (15)
	VATS	9 (70)
	RATS	2 (15)***

* Percentages may not always add up to 100 due to rounding to full numbers
** Multiple patients underwent combined lobectomy and wedge/segment resections
*** One converted to thoracotomy due to haemorrhage

N = number | LUMC = Leiden University Medical Centre | EMC = Erasmus Medical Centre | CEA = carcinoembryonic antigen IQR = interquartile range | RUL = right upper lobe | ML = middle lobe | RLL = right lower lobe | LUL = left upper lobe | LLL = left lower lobe | VATS = video assisted thoracic surgery | RATS = robot assisted thoracic surgery

TUMOUR LESIONS

Eighteen CLM were resected. Characteristics of all lesions are described in Table 2. *In vivo* imaging was performed on 16 lesions, back table imaging on 15 lesions, and closed-field imaging on 18 lesions. A positive fluorescence signal was observed in five lesions (31%) *in vivo*, in seven lesions (47%) with back table imaging and in 17 lesions (94%) with the closed-field imaging. Median SBRs for the three imaging modalities were 1.00 (IQR: 1.00-1.53), 1.45 (IQR: 1.00-2.05) and 4.81 (IQR: 2.70-7.41) respectively. All metastases were detected based on preoperative imaging and white light inspection. No lesions were identified solely based on NIR fluorescence imaging. Five metastases were located > 14 mm of the pleura, none of which showed positive *in vivo* fluorescence (median SBR: 1.00, range 1.00-1.34). For lesions ≤ 14 mm of the pleura, 5 out of 11 (45%) were fluorescent *in vivo* (median SBR: 1.34, range: 1.00-2.15) and 6 out of 11 (64%) lesions on the back table (median SBR: 1.98, range 1.00-3.53). Figure 1 presents an example of *in vivo* and back table imaging (lesion 7).

FIGURE 1 Representative in (A,B) and *ex vivo* (C, D, E, F) fluorescence images of a colorectal lung metastasis (lesion 7).
White light (left panels) and gradient fluorescence overlay (right panels) images.

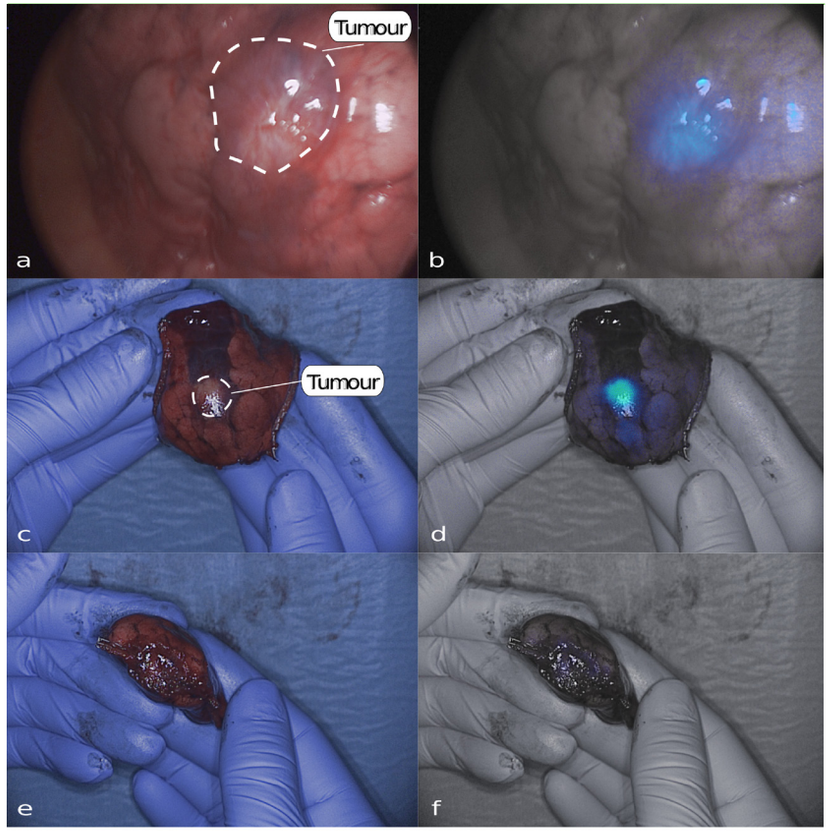

TABLE 2 Characteristics per lesion.

				Preoperative			Intraoperative			Pathology				IHC		
ID	Dose SGM-101	Lesion	Location	Distance to pleura (MM)	CT	WL	SBR (*in vivo*)*	SBR (*ex vivo*)*	Histopathology	Margin (MM)	SBR (bread loaf)*	Concordance **	IS	PS	TIS
1	7.5	1	RLL	6	+	+	2.15	MISS	metastasis CRC	4	6.1	TP	3	4	12
		2	station 11	N/A	-	+	1	MISS	benign LN	N/A	MISS	TN	N/A	N/A	N/A
		3	RLL	17	+	-	1.34	MISS	metastasis CRC	20	5.91	TP	3	4	12
2	7.5	4	RUL	10	+	+	1.62	3.53	metastasis CRC	5	6.43	TP	3	4	12
3	7.5	5	LLL	0	+	+	1.51	1.98	metastasis CRC	10	4.09	TP	3	4	12
		6	LLL	18	+	+	1	1.57	metastasis CRC	23	5.07	TP	3	4	12
4	10	7	RLL	22	+	+	MISS	MISS	metastasis CRC	2	10.44	TP	3	4	12
5	10	8	LUL	0	+	+	1.61	2.19	metastasis CRC	free	4.54	TP	3	4	12
6	10	9	RUL	8	+	+	1	1	fibrosis	N/A	MISS	TN	N/A	N/A	N/A
		10	RUL	2	+	+	1	1	fibrosis	N/A	MISS	TN	N/A	N/A	N/A
		11	RUL	N/A	-	+	1	1	fibrosis	N/A	MISS	TN	N/A	N/A	N/A
		12	RLL	23	+	+	1	1	metastasis CRC	3	1.52	TP	3	4	12
		13	ML	0	+	+	1	1	metastasis CRC	5	2.35	TP	3	4	12
7	12.5	14	RLL	3	+	+	1.34	1.19	metastasis CRC	6	2.99	TP	3	4	12
		15	ML	1	+	+	1	1	metastasis CRC	1	2.01	TP	3	4	12
		16	RUL	15	+	+	1	1	metastasis CRC	10	1.23	FN	3	4	12
		17	station 11	N/A	-	+	MISS	1	benign LN	N/A	MISS	TN	N/A	N/A	N/A
8	12.5	18	RUL	9	+	+	MISS	1.45	metastasis CRC	26	9.93	TP	3	4	12
9	12.5	19	RLL	7	+	-	1	2.04	metastasis CRC	free	3.8	TP	3	4	12
10	7.5	20	LUL	20	+	+	1	1	metastasis CRC	10	8.06	TP	3	4	12
11	7.5	21	LUL	10	+	+	1	2.13	metastasis CRC	free	9.88	TP	3	4	12
12	12.5	22	RUL	2	+	+	1	1.37	metastasis CRC	free	2.49	TP	3	4	12
13	10	23	LLL	0	+	+	1.6	2.06	metastasis CRC	free	7.73	TP	3	4	12
		24	station 7	N/A	-	+	MISS	1	benign LN	N/A	miss	TN	0	0	0
		25	station 8	N/A	-	+	MISS	1.78	malignant LN	N/A	miss	TP	3	4	12
		26	station 9	N/A	-	+	MISS	1	benign LN	N/A	miss	TN	N/A	N/A	N/A
		27	station 10	N/A	+	+	MISS	1.63	malignant LN	N/A	miss	TP	3	4	12
		28	station 11 ventral	N/A	+	+	1.59	1.69	malignant LN	N/A	miss	TP	3	4	12
		29	station 11 dorsal	N/A	-	+	MISS	1	benign LN	N/A	miss	TN	N/A	N/A	N/A

* an SBR of ≥ 1.5 is considered fluorescence positive ** concordance between fluorescence imaging and histopathology. Abbreviations: IHC = *immunohistochemistry* | MM = *millimetre* | CT = *computed tomography* | WL = *white light suspect* | SBR = *signal-to-background ratio* | IS = *intensity score* | PS = *proportion score* | TIS = *total immunostaining score* | RLL = *right lower lobe* | MISS = *missing* | CRC = *colorectal cancer* | TP = *true positive* | N/A = *not applicable* | LN = *lymph node* | TN = *true negative* | RUL = *right upper lobe* | LLL = *left lower lobe* | LUL = *left upper lobe* | ML = *middle lobe* | FN = *False negative*

LYMPH NODES

In patient 1 and 7, two benign lymph nodes were resected based on white light suspicion, but were fluorescence-negative (true negatives). In patient 13, a lymphadenectomy was performed for preoperatively identified hilar lymph node metastases. Three malignant lymph nodes were fluorescent on the back table (lesions 25, 27, 28, true positives). Three other non-fluorescent lesions were resected based on clinical suspicion for tumour involvement. All three contained fibrosis without tumour (lesions 24, 26, 29, true negatives). Figure 2 presents the white light and gradient overlay fluorescence images of three lymph nodes (lesions 25, 26, 28).

SGM-101 DOSE

Five patients (seven lesions) were injected with 7.5 mg SGM-101, four patients (five lesions) with 10 mg, and four patients (six lesions) with 12.5 mg. Median SBRs (closed-field imaging) for the dose levels were 6.1 (IQR: 5.50-7.25), 4.54 (IQR: 2.35-7.73), and 2.9 (IQR: 2.13-4.25) respectively (Figure 3a, p=0.20). There was no difference in absolute tumour or background mean fluorescence intensity (MFI) between the three dose groups (tumour: p=0.14, background: p=0.34, Figure 3b).

POTENTIAL CHANGE IN SURGICAL MANAGEMENT

In one patient, three clinically suspect, *in vivo* non-fluorescent nodules were resected (true negatives, lesions 9, 10, 11). In patient 5, the surgeon was unsure whether a complete removal of the tumour was achieved. Therefore, a small additional resection was performed. Fluorescence back table imaging of the primary specimen showed no tumour involvement of the resection margin (Figure 1, e and f). Final pathology assessment of primary resected specimen confirmed absence of tumour in the resection margin. In patient 9, tumour identification was based on the location on the CT scan and white light inspection. After resection, it was unclear whether the tumour was in the specimen, as the nodule was not palpable. After removing the staples, a clear fluorescent signal was observed in the specimen (Figure 4). The fluorescent tissue was sent for frozen section analysis and confirmed as malignant.

FIGURE 2 Fluorescence images of of malignant (A-D) and benign (E,F) lymph nodes.
White light (left panels) and gradient fluorescence overlay (right panels) images

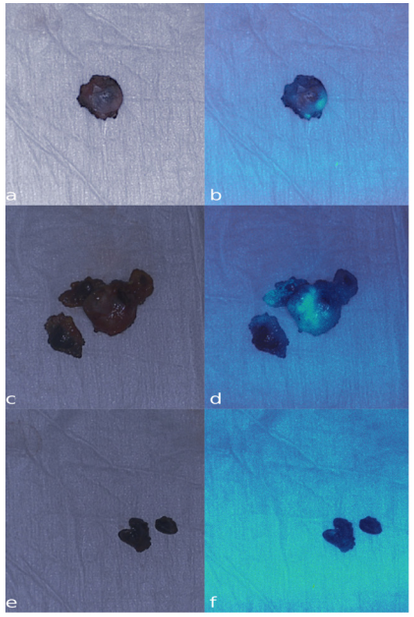

FIGURE 3 The signal-to-background ratios (A) and the mean fluorescence intensities (MFI) for tumour and background tissue per dose group (B) per dose group.
The boxes represent medians with q1 and q3 and the error bars represent the range.

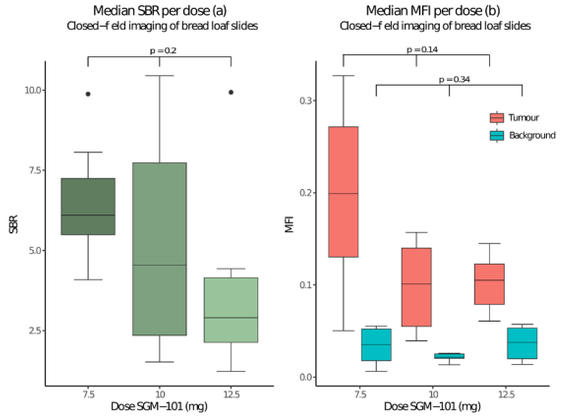

FIGURE 4 Images of an invisible and non-palpable tumour with a clear fluorescence signal (lesion 19).
White light (a) and gradient fluorescence overlay (b) images

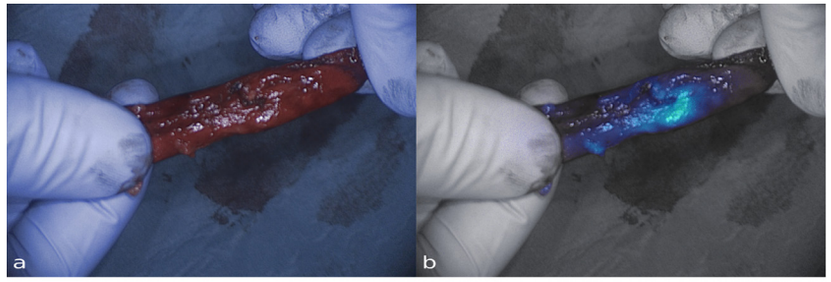

Preoperative serum CEA levels were elevated (> 5.0 µg/L) in 6 out of 11 patients and unknown in the other two patients. CEA expression of all 18 tumor lesions was assessed by immunohistochemistry and all 18 lesions had a total immunostaining score (TIS) of 12 out of 12. Figure 5 presents a bread loaf tissue section of a CLM imaged with several imaging modalities. Figure 6 presents a slide from the same tissue block with the H&E and CEA immunohistochemistry staining. Three tumor containing lymph nodes had maximum CEA expression (TIS: 12). One normal control lymph node had no CEA expression (lesion 24, TIS: 0). CEA expression per lesion is shown in Table 2.

FIGURE 5 A tissue slide of a CLM imaged with the PEARL MSI and Odyssey CLx scanner.

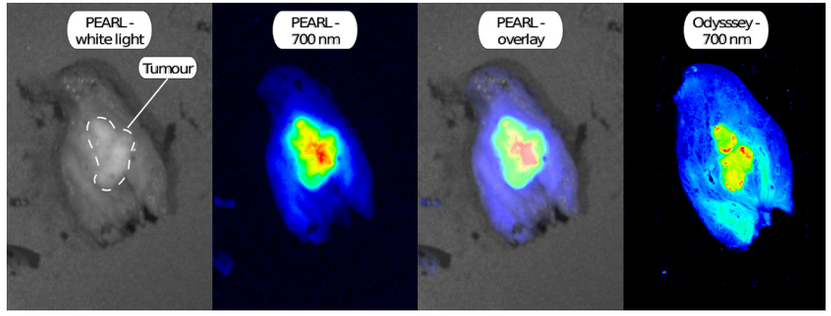

FIGURE 6 H&E staining and CEA immunohistochemistry staining on a tissue slide as demonstrated in Figure 5.

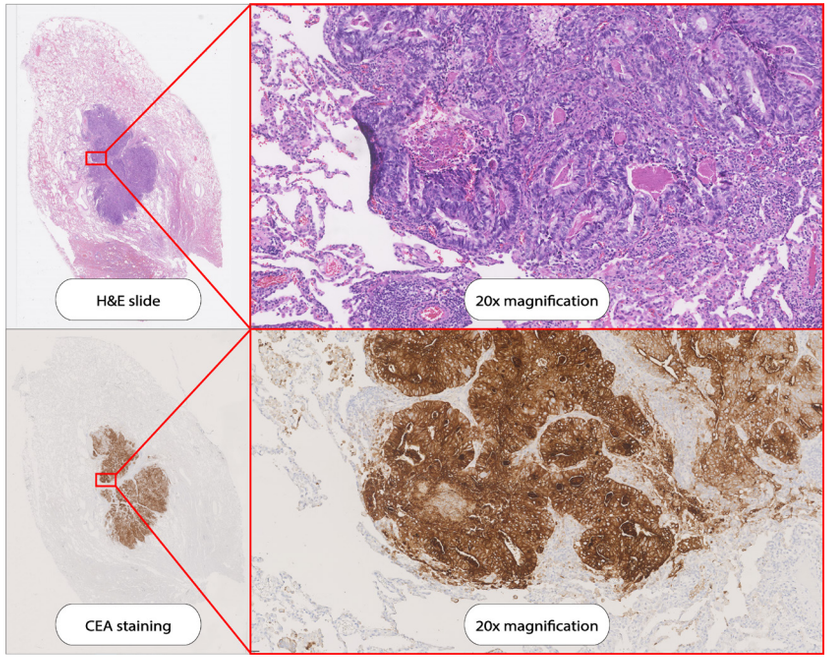

The present study shows that targeting of SGM-101 to CLM was accurate and that CEA is the target of choice for tumour-specific imaging of CLM. Challenges remain with *in vivo* detection of the tumour lesions, especially with the minimally invasive NIR fluorescence imaging system. The full potential of SGM-101 for *in vivo* detection of the tracer may therefore be achieved with improved minimally invasive imaging systems. Optimal patient selection may also further improve the efficacy of SGM-101. If intraoperative identification of the lesion is expected to be challenging, SGM-101 may help for the detection of superficial lesions. Identification of lesions deeper in the lung parenchyma is not expected to be possible with the technique, as overlying lung tissue negatively affects the observed fluorescence signal. An earlier study found a distance from the tumour to pleura of 14 mm as determined by pre-operative CT, to be the maximum tumour depth that can be imaged with an 800 nm fluorophore.[18] For SGM-101 (700 nm) this might be slightly lower.[5,19] In the current study, five lesions had a distance to the pleura of more than 14 mm on CT and none of these were fluorescent *in vivo*. A second application of intraoperative NIR fluorescence imaging is margin assessment. When close or positive resection margins are expected during surgery (e.g. when the tumour infiltrates the chest wall or a bronchus), intraoperative fluorescence imaging with SGM-101 may also be beneficial. For margin assessment, tumour depth is not influential. This is due to the fact that margin assessment is performed by imaging of the resection margin on the specimen on the back table. When positive margins are suspected, the wound bed can also be imaged to assess for residual signal. Given that 94% of the tumour bread loaves showed a positive fluorescence signal, it is expected that when tumour positive margins occur, they can be detected with this technique. Thus, patients with superficial nodules which are expected to be challenging to identify, or patients with tumours with potential tumour positive margins are most likely to benefit from the use of SGM-101.

A secondary objective of this study was to find the optimal dose of SGM-101 for the identification of CLM. For primary colorectal cancer, a dose of 10 mg was found to be the optimal dose.[10] Our study assessed three doses. In all dose groups sufficient SBRs were found. SBRs appeared to decrease with increasing doses but these differences were not significant. Therefore, a dose of 7.5 mg may be sufficient for pulmonary CLM imaging. The lowest dose is also preferable with regard to costs.

Recently, the first results were published on the use of SGM-101 for CLM and primary lung tumours.[20] In this study, ten patients were included, of which four had CLM. A dose of 10 mg of SGM-101 was administered according to the standard dose for primary or recurrent colorectal cancer. In the paper, only SBRs from the closed-field imaging were reported. When comparing SBRs from this trial to our results we find similar results, with mean SBRs of 3-4. For primary lung cancer surgery, several trials have been performed with other fluorescent tracers.[4] OTL-38 is a folate-α targeted fluorescent tracer for pulmonary adenocarcinoma that has been used in several studies for intraoperative imaging of primary lung adenocarcinoma. However, OTL-38 is not a good candidate for imaging of most other adenocarcinomas, including CRC. Less than 30% of the CRCs express folate-α, while CEA is expressed on 95% of tumours.[7,21,22]

Several limitations of this study can be mentioned. The low number of patients might have affected dose finding. In addition, patients were not selected based on tumour location and distance to the pleura. This may explain why several nodules were not fluorescent when imaged intraoperatively. However,

as we asked all eligible patients for participation, we most likely included a clinically representative cohort of patients.

In conclusion, the present study demonstrates the potential of fluorescence imaging of CLM with SGM-101. Closed-field imaging of bread loaves showed excellent targeting of the tracer to the tumour nodules, with maximum target expression on all tumour nodules. Challenges remain with *in vivo* detection of this tracer. Improving minimally invasive fluorescence imaging systems and optimal patient selection most likely enables the optimal efficacy of SGM-101 for CLM surgery.

REFERENCES

1 Meyer Y Olthof PB Grünhagen DJ de Hingh I de Wilt JHW Verhoef C et al. Treatment of metachronous colorectal cancer metastases in the Netherlands: A population-based study. Eur J Surg Oncol. 2021.

2 Riihimäki M Hemminki A Sundquist J Hemminki K. Patterns of metastasis in colon and rectal cancer. Sci Rep. 20166:29765.

3 Hao Z Parasramka S Chen Q Jacob A Huang B Mullett T et al. Neoadjuvant Versus Adjuvant Chemotherapy for Resectable Metastatic Colon Cancer in Non-academic and Academic Programs. Oncologist. 2022.

4 Neijenhuis LKA de Myunck L Bijlstra OD Kuppen PJK Hilling DE Borm FJ et al. Near-Infrared Fluorescence Tumour-Targeted Imaging in Lung Cancer: A Systematic Review. Life (Basel). 202212.

5 Keereweer S Van Driel PB Snoeks TJ Kerrebijn JD Baatenburg de Jong RJ Vahrmeijer AL et al. Optical image-guided cancer surgery: challenges and limitations. Clin Cancer Res. 201319:3745-54.

6 Gutowski M Framery B Boonstra MC Garambois V Quenet F Dumas K et al. SGM-101: An innovative near-infrared dye-antibody conjugate that targets CEA for fluorescence-guided surgery. Surg Oncol. 201726:153-62.

7 Tiernan JP Perry SL Verghese ET West NP Yeluri S Jayne DG et al. Carcinoembryonic antigen is the preferred biomarker for *in vivo* colorectal cancer targeting. Br J Cancer. 2013108:662-7.

8 Meijer RPJ de Valk KS Deken MM Boogerd LSF Hoogstins CES Bhairosingh SS et al. Intraoperative detection of colorectal and pancreatic liver metastases using SGM-101 a fluorescent antibody targeting CEA. Eur J Surg Oncol. 202147:667-73.

9 Schaap DP de Valk KS Deken MM Meijer RPJ Burggraaf J Vahrmeijer AL et al. Carcinoembryonic antigen-specific fluorescent image-guided cytoreductive surgery with hyperthermic intraperitoneal chemotherapy for metastatic colorectal cancer. Br J Surg. 2020107:334-7.

10 de Valk KS Deken MM Schaap DP Meijer RP Boogerd LS Hoogstins CE et al. Dose-Finding Study of a CEA-Targeting Agent SGM-101 for Intraoperative Fluorescence Imaging of Colorectal Cancer. Ann Surg Oncol. 202128:1832-44.

11 Hoogstins CES Boogerd LSF Sibinga Mulder BG Mieog JSD Swijnenburg RJ van de Velde CJH et al. Image-Guided Surgery in Patients with Pancreatic Cancer: First Results of a Clinical Trial Using SGM-101 a Novel Carcinoembryonic Antigen-Targeting Near-Infrared Fluorescent Agent. Ann Surg Oncol. 201825:3350-7.

12 Boogerd LSF Hoogstins CES Schaap DP Kusters M Handgraaf HJM van der Valk MJM et al. Safety and effectiveness of SGM-101 a fluorescent antibody targeting carcinoembryonic antigen for intraoperative detection of colorectal cancer: a dose-escalation pilot study. Lancet Gastroenterol Hepatol. 20183:181-91.

13 Vahrmeijer AL. SGM-101 in Locally Advanced and Recurrent Rectal Cancer (SGM-LARRC). ClinicalTrial.gov.

14 Vahrmeijer AL. Performance of SGM-101 for the Delineation of Primary and Recurrent Tumour and Metastases in Patients Undergoing Surgery for Colorectal Cancer. ClinicalTrials.gov.

15 Azargoshasb S Boekestijn I Roestenberg M KleinJan GH van der Hage JA van der Poel HG et al. Quantifying the Impact of Signal-to-background Ratios on Surgical Discrimination of Fluorescent Lesions. Mol Imaging Biol. 2022.

16 Lauwerends LJ van Driel P Baatenburg de Jong RJ Hardillo JAU Koljenovic S Puppels G et al. Real-time fluorescence imaging in intraoperative decision making for cancer surgery. Lancet Oncol. 202122:e186-e95.

17 Linders D Deken M van der Valk M Tummers W Bhairosingh S Schaap D et al. CEA EpCAM αvβ6 and uPAR Expression in Rectal Cancer Patients with a Pathological Complete Response after Neoadjuvant Therapy. Diagnostics (Basel). 202111.

18 Okusanya OT Holt D Heitjan D Deshpande C Venegas O Jiang J et al. Intraoperative near-infrared imaging can identify pulmonary nodules. Ann Thorac Surg. 201498:1223-30.

19 Kennedy GT Azari FS Chang A Nadeem B Bernstein E Segil A et al. Comparative Experience of Short Versus Long Wavelength Fluorophores for Intraoperative Molecular Imaging of Lung Cancer. Ann Surg. 2022.

20 Azari F Meijer RPJ Kennedy GT Hanna A Chang A Nadeem B et al. Carcinoembryonic Antigen-Related Cell Adhesion Molecule Type 5 Receptor-Targeted Fluorescent Intraoperative Molecular Imaging Tracer for Lung Cancer: A Nonrandomized Controlled Trial. JAMA Netw Open. 20236:e2252885.

21 D'Angelica M Ammori J Gonen M Klimstra DS Low PS Murphy L et al. Folate receptor-α expression in resectable hepatic colorectal cancer metastases: patterns and significance. Mod Pathol. 201124:1221-8.

22 Chen CI Li WS Chen HP Liu KW Tsai CJ Hung WJ et al. High Expression of Folate Receptor Alpha (FOLR1) is Associated With Aggressive Tumour Behavior Poor Response to Chemoradiotherapy and Worse Survival in Rectal Cancer. Technol Cancer Res Treat. 202221:15330338221141795.